International Journal of Refrigeration 145 (2023) 264–275

Contents lists available at ScienceDirect

International Journal of Refrigeration

journal homepage: www.elsevier.com/locate/ijrefrig

Performance analysis of heat pumps with zeotropic mixtures at different load conditions

Andreas Søgaard Kristensen [a,1], Emil Kruse Sørensen [a,1], Claus Madsen [b], Jóhannes Kristófersson [b], Pourya Forooghi [a,*]

[a] Department of Mechanical & Production Engineering, Aarhus University, Inge Lehmans Gade 10, Aarhus C, 8000, Denmark
[b] Danish Technological Institute, Gregersensvej 1, Taastrup, 2630, Denmark

ARTICLE INFO

Keywords:
Heat pump
Zeotropic mixtures
Off-design performance
Temperature glide
District heating

ABSTRACT

Heat pump cycles with zeotropic mixtures as working fluids and temperature glides on both heat sink and heat source sides are analyzed. Five binary zeotropic mixtures, selected based on previous studies in the literature, are examined. The cycles are initially optimized for each binary mixture at three different heat source temperature glides (10–30 K) and fixed heat sink temperature glide (30 K). The variation in the heating COP of the optimized designs is then computed and compared for five different part load scenarios down to 40% of the design point heating load. The design point optimization is performed for different single and double-compression cycle layouts, based on which the standard vapor compression cycle with a suction gas heat exchanger is adopted as the most economical option for the rest of the study. The part load cycle simulations demonstrate that, when the heat source temperature glide is large, two of the studied part load scenarios can lead to increased COP; these are when the reduction in the heating load is due to (1) an increase in both the heat sink (e.g. district heating water) inlet and heat source (e.g. process water) outlet temperatures, and (2) a decrease in both heat sink and source flow rates. Moreover, it is observed that different mixtures show different levels of sensitivity to a decrease in heating load. Among the studied mixtures, DME/Iso-Pentane while outperforming others in all studied cases, has the most unfavorable trend at part load, hence losing its benefit margin over other candidates.

1. Introduction

As a part of global effort towards sustainable energy utilization, interest in heat pumps has increased in recent years. Special attention has been paid to the heat pumps with large temperature glides on the sink and source sides — an attempt to electrify the heat supply in applications previously relying on non-renewable energy resources, e.g. in the process industry (Barco-Burgos et al., 2022). Such heat pumps are also attractive options in waste heat recovery, where one process can be utilized to heat another process or the water in a district heating network (Tan et al., 2021).

It is well known that a Lorenz-based cycle can deliver an improved performance compared to a single Carnot cycle when the heat sink and source of the heat pump have variable temperatures (Radermacher and Hwang, 2005). The basis of the Lorenz cycle is a working fluid that perfectly matches the sink and source temperature profiles. This leads to a decrease in exergy destruction in the heat exchangers (Zühlsdorf et al., 2018a). Such a working fluid therefore, needs to have a non-isothermal phase change, which is a characteristic of zeotropic mixtures; what has served as a basis for increased interest in zeotropic mixtures as working fluids in recent years. In a zeotropic mixture, the magnitude of temperature glide – the temperature difference between saturated gas and saturated liquid – depends on the mass fraction of its components and can vary significantly depending on the composition (Rajapaksha, 2007).

To comply with the environmental and safety regulations in terms of the Montreal protocol (United Nations, 1987) and the Kyoto protocol (United Nations, 1998) many established working fluids are phased out and focus has turned towards non-toxic working fluids with low global warming potential (GWP) and zero ozone depletion potential (ODP). This points toward the use of natural refrigerants in zeotropic mixtures. Furthermore, a non-flammable working fluid or one with low flammability reduces the safety measures to be observed.

* Corresponding author.
E-mail addresses: andreas5910@hotmail.com (A.S. Kristensen), emil_soerensen@hotmail.com (E.K. Sørensen), clma@vestfor.dk (C. Madsen), jkri@teknologisk.dk (J. Kristófersson), forooghi@mpe.au.dk (P. Forooghi).
[1] First and second authors contributed equally to this work.

https://doi.org/10.1016/j.ijrefrig.2022.09.028
Received 22 May 2022; Received in revised form 13 September 2022; Accepted 28 September 2022
Available online 17 October 2022

Nomenclature

α	Convective heat transfer coefficient [W/(m^2 K)]
ΔT_m	Mean temperature difference in heat exchangers [K]
A	Heat transfer area [m^2]
f	Reduction factor [–], defined by Eq. (6)
Q	Heat transfer [kW]
q	Heat flux [W/m^2]
U	Overall heat transfer coefficient [W/(m^2 K)]
COP	Coefficient of performance
DCC	Double compression cycle
DCC-SGHX	Double compression cycle with suction gas heat exchanger
DME	Dimethyl ether
GWP	Global warming potential
HC	Hydro carbon
ODP	Ozone depletion potential
ODPR	Optimum design point mass fraction ratio
PL	Part Load Scenario
SC-SGHX	Standard cycle with suction gas heat exchanger
SGHX	Suction gas heat exchanger
VHC	Volumetric heating capacity [kJ/(m^3 K)]

Subscripts

cond	Condenser
DP	Design point
evap	Evaporator
min	Minimum
pinch	Pinch point
PL	Part load
sep	Separator
sup	Superheat
WF	Working fluid

Consequently, several researchers (e.g. Mohanraj et al., 2011; Dai et al., 2015; Zühlsdorf et al., 2018c; Yelishala et al., 2020b) conduct screenings of possible working fluids fulfilling these requirements. They especially recommend natural fluids in terms of different hydrocarbons (HC) as possible replacements. Among various candidate working fluids, some such as Dimethyl Ether (DME), Propylene, Propane, Butane, Iso-Butane and Iso-Pentane has received attention in all these studies. Moreover, all these studies consider CO_2 as the flame suppressant fluid in a mixture. More recently, Wang et al. (2020b, 2021) conduct studies showing that increasing the amount of CO_2 in a mixture decreases the flammability. Yu et al. (2018) clarify the fraction of CO_2 in the mixture needed to reach different safety classes.

In view of the above facts, zeotropic mixtures of natural refrigerants can be considered as attractive working fluid options when there is a temperature glide in the heat sink and/or source of the cycle. This is not the case at constant heat sink/source temperatures as demonstrated by Yelishala et al. (2020b) and Sarkar and Bhattacharyya (2009), who study basic refrigeration cycles and compare different mixtures to pure fluids and, in all cases, recommend pure fluids. However, another study by Yelishala et al. (2020a), in which the same mixtures as in Yelishala et al. (2020b) are investigated, shows that mixtures outperform the pure fluids where there are temperature glides. This finding is systematically confirmed in a number of studies by Zühlsdorf et al. (2018c,a, 2019). Specifically, Zühlsdorf et al. (2018a) optimized the performance of binary zeotropic mixtures combined by 14 natural refrigerants at different temperature combinations. These authors show that with large temperature glides on the source (15 K and 20 K) the mixtures significantly outperform the pure fluids. Kim et al. (2008) used experiments to demonstrate that a considerable enhancement in COP can be achieved if the temperatures glides are appropriately matched by the working fluid and a sufficient heat exchanger area is present. Other researchers (e.g. Guo et al., 2019; Park and Jung, 2009) report results in line with the ones mentioned. When it comes to CO_2-based mixtures, Zhang et al. (2017) suggest the combination CO_2/Propane to be the most promising refrigerant option.

While a majority of studies focus on simple vapor compression cycles, certain authors examine combinations of mixtures with more advanced cycle architectures. For instance, Jung et al. (1999) and Wang et al. (2020a) investigate a two-stage compression cycle and show that using a multistage heat pump with appropriate mixtures, it is possible to achieve a significant increase in the COP compared to that of a single stage heat pump using pure refrigerants. However, unlike the present study, the focus of these authors is on azeotropic or non-HC mixtures. Shariatzadeh et al. (2016) compare supercritical CO_2 system with expander and expansion valve with and without suction gas heat exchanger (SGHX) and reported that a system with an expander and without SGHX has the highest performance. Based on a comprehensive comparison in which several cycle options including multistage systems are included, Sarkar (2010) recommends the ejector as the most optimum addition to the simple cycle in terms of cost–benefit trade-off. While the Shariatzadeh et al. (2016), Sarkar (2010) study expanders and ejectors for a supercritical CO_2 system, a study combining ejector and mixtures is performed by Brodal and Eiksund (2020). In this study, a single-stage CO_2/Propane cycle with an ejector is compared to one with and without a SGHX for a water-to-water heat pump. These authors optimize the performance of different cycles at different temperature cases and reveal that the ejector-based cycle generally performs better with pure fluids. The highest performance with mixtures is reported for a system containing an SGHX. Madsen et al. (2019) investigate different cycle layouts, many of which include the option of internal liquid circulation, aiming for a better temperature glide match in the heat exchangers. The results of this project, however, reveal that in most cases a simple cycle with an SGHX is the best performing system design in terms of COP.

The studies mentioned above, mainly address the design point performance, while in real-world applications there are multiple scenarios that can lead to part load operation. That is, for certain periods of operation, the conditions on either the sink or source side of a heat pump can be different from those for which it is designed. Depending on how the conditions of the source and sink change, this can impact the performance of the heat pump. Recently, Zühlsdorf et al. (2018c) investigated the performance of heat pumps with basic vapor compression cycle at part load for various zeotropic mixtures and show that mixtures have a better COP than pure fluids also at part load. These authors assume the overall heat transfer coefficient in heat exchangers to be the same at full and part load. A similar conclusion is achieved in the study by Xiao et al. (2020) where a double compressor cycle with an intermediate pressure vessel is investigated. In this study, however, an azeotropic mixture is used and the heat source has a constant temperature. Other researchers, e.g. Faegh and Shafii (2019) and Pieper et al. (2021), also study off-design performance of heat pumps, while Sahin and Adiguzel (2022) investigate the effects of climate conditions on a heat pump. All these works, however, deal with pure working fluids.

Despite the wealth of knowledge available on the performance of heat pumps with zeotropic mixtures, a limited attention has been paid to the part load performance and the existing literature on this subject mainly concerns limited number of scenarios and working fluids as discussed in the previous paragraphs and summarized in Table 1. This

Table 1
A summary of recent literature on heat pumps with mixtures and/or working at part load. The references dealing with part load, did not systematically study different part load scenarios, which is at the focus of the present work.

Ref.	Refrigerant	Source temperature	Sink temperature	Application	Part-load studied?
Zühlsdorf et al. (2018a)	Several mixtures incl. CO2/Propane Propylene/Butane Propylene/Isobutane DME/Isopentane Propane/Butane	40 °C → 35 °C 40 °C → 30 °C 40 °C → 25 °C 40 °C → 20 °C	40 °C → 80 °C	No specific	No
Yelishala et al. (2020a)	CO2/Propane CO2/Propylene CO2/Isobutane CO2/DME	30 °C → 15 °C	45 °C → 60 °C	Air-conditioning	No
Zühlsdorf et al. (2018c)	Several mixtures incl. DME/Isopentane Propylene/Isobutane	40 °C → 25 °C	40 °C → 60 °C	Booster heatpump	Yes (Constant UA-value)
Xiao et al. (2020)	R290/R600a/R1311	T_{evap} = 18 °C	T_{cond} = 85 °C	Air-conditioning	Yes
Faegh and Shafii (2019)	Unspecified pure refrigerant	T_{evap} = 14 °C T_{evap} = 8 °C T_{evap} = 2 °C	T_{cond} = 40 °C	Air humidification -dehumidification desalination system	Yes
Pieper et al. (2021)	Ammonia	7 °C → 1 °C 4 °C → 1 °C 16 °C → 6 °C	60 °C → 85 °C	District heating	Yes

Table 2
Mixtures analyzed in this study.

	Component 1	Component 2
1	Propylene	Iso-Butane
2	Propylene	Butane
3	Propane	Butane
4	DME	Iso-Pentane
5	CO_2	Propane

Table 3
Temperature cases for the design conditions.

Temperature cases	1	2	3
$T_{source.in}$ [°C]	40	30	20
$T_{source.out}$ [°C]	10	10	10
$T_{sink.in}$ [°C]		40	
$T_{sink.out}$ [°C]		70	

calls for a comprehensive and systematic research campaign, to which the present work attempts to contribute. We are particularly interested in answering the following questions: do mixtures show a superior performance over pure working fluids at large temperature glides also when operating at different part load scenarios? Are there any part load scenarios that are favorable for mixture-based heat pumps? Are the optimal mixture compositions the same at both design point and part load operating conditions? Apart from limited research on part load performance, the existing literature on zeotropic mixtures has been less concerned with double compression cycles. Therefore, the present work is also partly devoted to the possibility of performance improvement using cycles with intermediate pressure vessels.

The paper is organized as follows. In Section 2, the cycle architectures, study cases and simulation and optimization methodologies are described. In Section 3, the results of the study are presented. First, we compare different cycle architectures 'optimized for the design point' conditions. Here three cycles are compablack, one with SGHX and without intermediate pressure vessel, one with intermediate pressure vessel and without SGHX, and a third one with both. In the second part of Section 3, we investigate the performance of selected cycles at different 'part load' scenarios, in which the temperatures and/or mass flow rates of the sink and source streams are systematically varied. The main findings of the paper are summarized in Section 4.

2. Methodology

In this section, the cycle architectures and operating conditions of interest as well as the procedures of design point optimization and the part load simulations are described.

The analysis is focused on selected mixtures listed in Table 2. These consist only of natural refrigerants for the reasons outlined in the introduction. Moreover, the fluids are mainly hydrocarbons except for CO_2 in mixture 5, which is included as a potential flame suppressing agent (Yu et al., 2018). All other mixtures are flammable. Previous works by Zühlsdorf et al. (2018c,a, 2019) shows fluid mixtures 1–4 to have potential for very high COPs. The choice of mixing CO_2 and Propane is based on the findings made by Zhang et al. (2017). To summarize, the selected mixtures are

- all natural refrigerants,
- widely focused in the academic literature,
- shown to be proper candidates to match the type of temperature glides faced in typical heat pump applications, and
- (in case of CO_2) can be considered as a flame suppressant.

2.1. Design point optimization

In design point optimization, the performance in terms of COP for different cycle layouts is optimized for three Temperature Cases shown in Table 3. The choice for the heat sink temperatures is based on typical supply and return temperatures in district heating. Fig. 1 illustrates the three cycle layouts that are optimized. Note that the condenser is simply illustrated as one component while it can include a subcooler, a condenser and a desuperheater. Furthermore, in case of a supercritical cycle (which can be optimal for some CO_2/Propane mixtures) it represents a gas cooler.

The optimization has focus on performance in terms of COP for the three cycles. The COP for SC-SGHX is calculated as shown by Eq. (1).

$$COP_{SC.SGHX} = \frac{Q_{cond}}{P_{Comp}} \tag{1}$$

To calculate the COP for DCC and DCC-SGHX Eq. (2) is used

$$COP_{DCC} = \frac{Q_{cond}}{P_{CompH} + P_{CompL}} \tag{2}$$

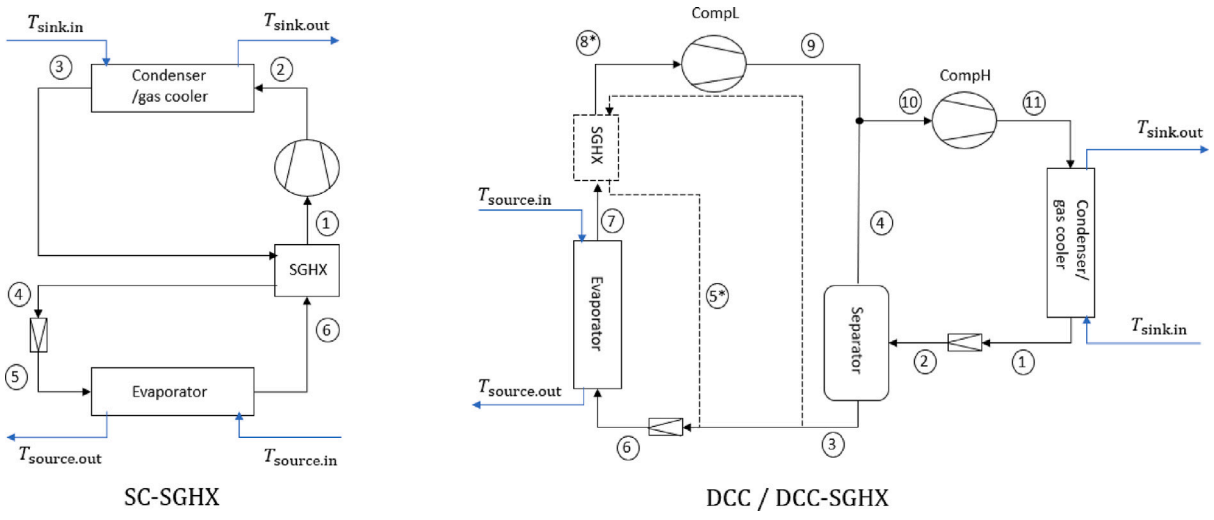

Fig. 1. Cycle layouts of heat pumps analyzed. On the left; the Standard Cycle with Suction Gas Heat Exchanger (SC-SGHX). On the right; Double Compressor Cycle (DCC) and Double Compressor Cycle with Suction Gas Heat Exchanger (DDC-SGHX). The difference between the DCC and DCC-SGHX is the inclusion of a suction gas heat exchanger (SGHX). Therefore DCC-SGHX has two more state points; 5* and 8*. The systems are simplified in terms of the condenser since it covers the subcooler, condenser and desuperheater.

2.1.1. Component modeling

To maintain the generality of the discussion, in both design-point optimization and part load analysis, we make generic assumptions with regard to the cycle components rather than focusing on specific components. The key assumptions are described in the following. In all cycles, the heat exchangers (condenser, evaporator and SGHX) are modeled as counter-flow heat exchangers and pressure drops are neglected. Following the approach proposed by Zühlsdorf et al. (2019), the heat exchangers are modeled with a required pinch temperature, $T_{pinch.min}$ of at least 4 K, which ensures the size of heat exchangers in the cycle to remain within a reasonable range. The compressors are modeled with a constant isentropic efficiency of $\eta_{comp.is} = 0.8$ independent of the working fluid mixture. One must keep in mind that constant efficiency is a common simplification. In reality the efficiency varies with the pressure ratio and working fluid. In the calculations, the enthalpy rise through the compressor Δh_{comp} is calculated by dividing the isentropic enthalpy rise with the same pressure ratio $\Delta h_{comp.is}$ by the efficiency $\eta_{comp.is}$. Typically, piston compressors are used in such systems. At the inlet of the separator (state 2 for DCC/DCC-SGHX in Fig. 1) the vapor quality cannot be lower than 0.02. This is implemented for simulation stability and also to ensure that the separator is indeed relevant. In the separator the gas and liquid phases are modeled to have the same temperature and pressure. The temperature for the condenser outlet is always set to be the pinch temperature above the sink inlet temperature. This has been defined to completely exploit subcooling, which leads to an increase in performance (Zühlsdorf et al., 2018a). Furthermore, it is required that the outlet of the condenser at least is saturated liquid when the system is subcritical. The outlet of the evaporator is defined as saturated gas except in the DCC cycle, where the superheating should be reached inside the evaporator. For the double compressor cycles, the outlets of the separator are also known since states 3 and 4 in Fig. 1 are always saturated liquid and saturated gas, respectively. For all cycles the expansion valve is modeled as isenthalpic.

Heat transfer rate in a heat exchanger (including condenser and evaporator) should follow Eq. (3)

$$Q = U A \Delta T_m \tag{3}$$

As will be explained later, part load calculation requires a knowledge of the value of UA at the design point for each heat exchanger. To this end we discretize the temperature profiles in flow direction into small segments, in each of which the following equation holds.

$$dQ = U\, dA \Delta T \tag{4}$$

Here ΔT and dQ are the temperature difference between the hot and cold fluids and heat transfer rate at the segment, respectively. The segments are chosen in a way that all have the same dQ (in other words the heat exchanger is discretized equidistantly along the enthalpy axis). As ΔT in each segment is also known from the temperature lines of the two streams, Eq. (4) can then be used to find UdA for the segment. The UA value for the entire heat exchanger is then the sum of the UdA values for all segments considering a uniform U along the heat exchanger as a first approximation. This quantity functions as a measure of the size of the heat exchangers.

2.1.2. Optimization

The systems are optimized with regard to different variables. For SC-SGHX, the amount of superheat entering the compressor (T_{sup}), condenser/gas cooler pressure (p_{cond}), and the evaporator pressure (p_{evap}) are the optimization variables. For the two cycles with the intermediate pressure vessel the separator pressure (p_{sep}) is an additional optimization variable. The superheat is constrained in the range of 10 K to 30 K due to different practical considerations; if the superheat is too low liquid droplets might be present at the outflow, which is harmful to the compressor. Some of the working fluids are also soluble with the oil used for lubricating the compressor. If dissolved in oil, the working fluid can change the properties of the oil – most importantly the viscosity – and negatively affect the lifetime of the compressor. On the other hand circulation of oil in the cycle can bring about problems such as deterioration of heat transfer in heat exchangers. A practical approach to mitigate this problem is maintaining a large level of superheat. Furthermore, it is noted that some mixtures have steep gas-saturation lines, in which case a large superheat helps avoid entering the two-phase area in the compressor. However, too large a superheat value also means that the density on the suction side of the compressor is too low.

An optimization routine in MATLAB ©, based on the framework proposed by Zühlsdorf et al. (2018b) for optimizing heat pumps working with zeotropic mixtures, is utilized. The global optimization routine Particle Swarm Optimization (PSO) is used from the Optimization Toolbox in MATLAB © (The MathWorks Inc., 2021). As PSO does not handle constraints explicitly these are implemented via penalty functions as described by Brodal and Eiksund (2020). The penalty function is chosen to be quadratic with fixed penalty parameters as described in Nocedal and Wright (2006). For example, the minimization problem for the

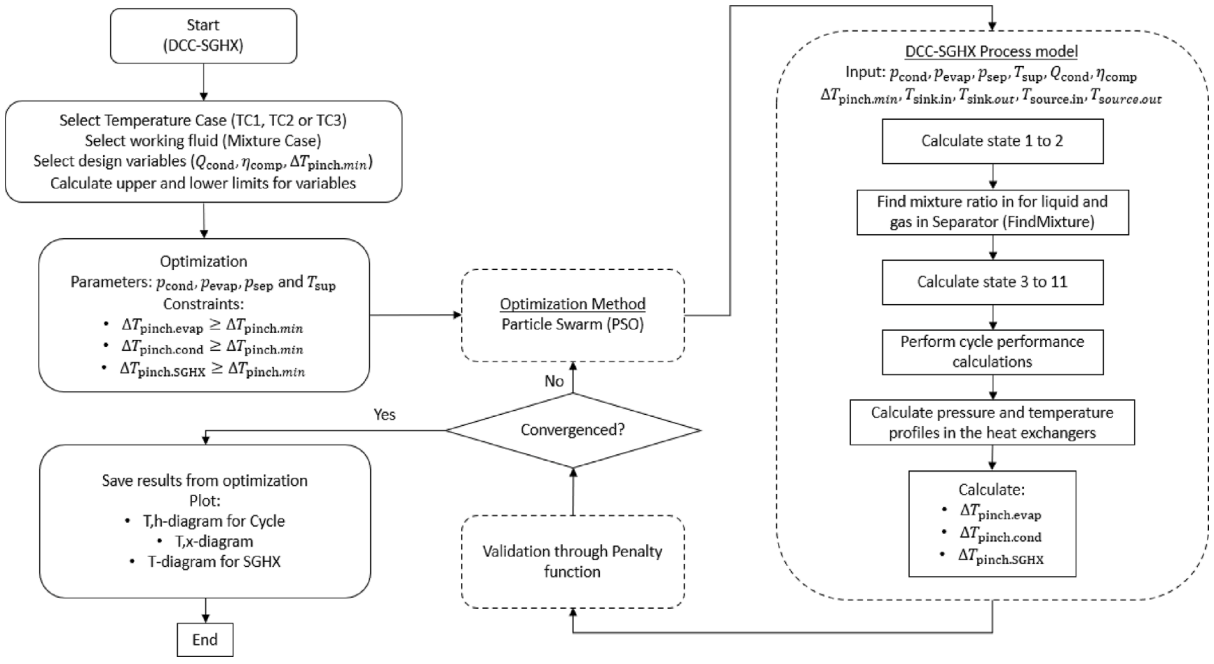

Fig. 2. Flowchart of the model used to optimize the different systems. It is here shown with DCC-SGHX as an example.

design point optimization of SC-SGHX is given by

$$\begin{aligned} q_{SC.SGHX} = &- \text{COP} \\ &+ k_1 \cdot [\max(0, \Delta T_{pinch.min} - \Delta T_{pinch.evap})]^2 \\ &+ k_2 \cdot [\max(0, \Delta T_{pinch.min} - \Delta T_{pinch.cond})]^2 \\ &+ k_3 \cdot [\max(0, \Delta T_{pinch.min} - \Delta T_{pinch.SGHX})]^2 \end{aligned} \quad (5)$$

In Eq. (5) $q_{SC.SGHX}$ is the objective function to be minimized, which includes the COP (with the negative sign due to minimization) and three constraints, each multiplied by a penalty factor k_i. When each of the constrained pinch temperature differences goes below the prescribed minimum value the respective term yields a larger value for the objective function, hence the optimization algorithm forces the constraint to be satisfied. The penalty factors can also be interpreted as Lagrange multipliers for the constrained optimization problem. Properties of the working fluid mixtures are found by REFPROP 9 (Lemmon et al., 2018) through an interface with MATLAB. The optimization routine is illustrated in Fig. 2.

2.2. Part load simulation

A working condition in which the heat load of the condenser/gas cooler is smaller than the design condition, for which the cycle is optimized, is referred to as part load. Part load performance of heat pumps and working fluid mixtures is important to investigate as it can have a significant impact on the overall performance of the heat pump system. Considering that the heat pumps are often expected to supply heating at a fixed temperature $T_{sink.out}$, part load operation can occur due to a change in the water return temperature $T_{sink.in}$ or mass flow rate $\dot{m}_{sink}$ in the condenser. In the present work, five different part load scenarios are studied, which are summarized in Table 4. The two above mentioned conditions on the sink side are combined with different possibilities for reducing the heat load on the source side (evaporator). To exemplify, consider PL1 in Table 4 combined with Temperature Case 1 from Table 3 with Q_{cond} being reduced to 40% of the design point load. As $T_{sink.in}$ is the only variable on the sink side in PL1, it will increase from 40 °C to 58 °C, so that $T_{sink.out} - T_{sink.in}$ and hence Q_{cond} reduce by 60%. This in turn leads to an increase in the source side inlet temperature $T_{source.in}$ in this scenario.

Table 4
Part Load Scenario (PL) for the source and sink.

Scenario	Source		Sink	
	Variable	Fixed	Variable	Fixed
PL1	$T_{source.in}$	$T_{source.out}$, $\dot{m}_{water}$		
PL2	$T_{source.out}$	$T_{source.in}$, $\dot{m}_{water}$	$T_{sink.in}$	$T_{sink.out}$, $\dot{m}_{water}$
PL3	$\dot{m}_{water}$	$T_{source.in}$, $T_{source.out}$		
PL4	$\dot{m}_{water}$	$T_{source.in}$, $T_{source.out}$	$\dot{m}_{water}$	$T_{sink.in}$, $T_{sink.out}$
PL5	$T_{source.in}$	$T_{source.out}$, $\dot{m}_{water}$		

Overall, the goal is to understand how zeotropic mixtures behave at different part load scenarios and if there are any scenarios that are particularly undesirable for mixtures in comparison to pure working fluids. As mentioned, in all part load scenarios, the sink outlet temperature (e.g. district heating supply temperature) is kept constant.

The variables in this simulation are different from the ones used in the Design Point Optimization. The pressures are still variables but the superheat entering the compressor is fixed at the design point value. This is a result of the way the heat pump is controlled to have a fix superheat temperature. Instead, the amount of subcooling at the condenser outlet is a variable since the degree of subcooling can vary with varying heat loads. Furthermore, the evaporator outlet enthalpy is also a variable, as the working fluid can exit the evaporator both as two-phase but also as superheated. This is since the system is simulated as if the temperature sensor for the expansive valve is placed between the compressor and SGHX.

It is important to note that the aim here is not to optimize the heat pump for the highest COP, but rather to assess the same heat pump at new operating conditions corresponding to part load. In other words, we simulate the steady-state of the systems at new values of water temperatures and/or mass flow rate at sink and source. The size of heat exchangers at full and part load is the same. In our simulation determining ΔT_m in each heat exchanger requires an estimation of the *UA*-value, which is explained in the following subsection. Once ΔT_m at the system's new steady-state is determined, it is enforced using the PSO algorithm with a penalty function similar to Eq. (5).

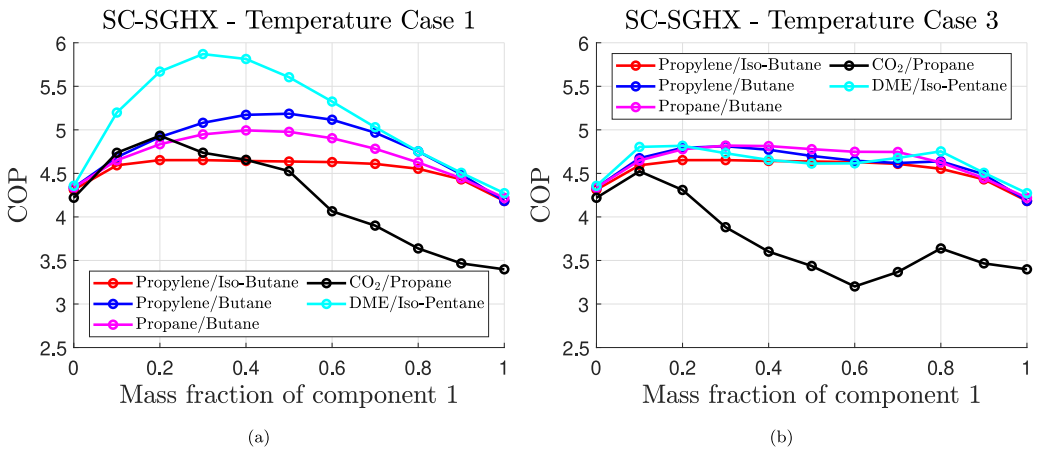

Fig. 3. Optimized COP for SC-SGHX for Temperature Cases 1 and 3. The data for temperature case 2, not shown for brevity, lie in between those of the shown cases. The source temperature varies from 40 °C to 10 °C (Case 1) and 20 °C to 10 °C (Case 3). The sink temperature varies from 40 °C to 70 °C in all cases. Component 1 is the first fluid in the mixture name. The COP at mass fractions of 1 and 0 correspond to the COP of the first and second component in the pure form, respectively.

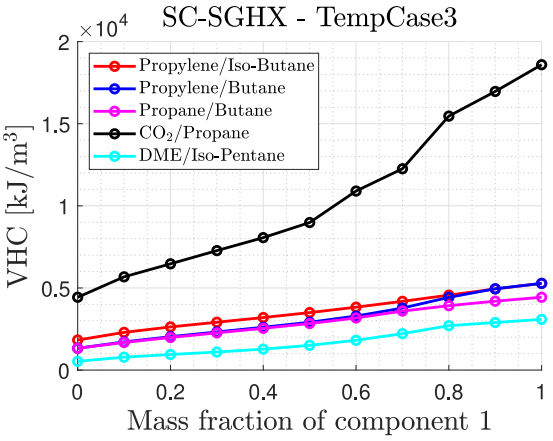

Fig. 4. The volumetric heating capacity (VHC) for all mixtures with different compositions. The values are calculated based on results for Temperature Case 3 in Table 3.

2.2.1. Heat exchangers

At part load, the heat load in the condenser is reduced, which causes a reduction in the mass flow rate of the working fluid. Furthermore as shown in Table 4, the mass flow rate of water may decrease in certain scenarios. Since the flow cross section in the heat exchanges is identical to the one at the design point, this is assumed to lead to a decrease in velocity of either or both fluids, which results in lower heat transfer coefficients in the heat exchanger depending on the scenario. Lower heat transfer coefficients cause a lower U. We define a factor f ($0 \leq f \leq 1$) to represent reduction in U in part load:

$$U_{\mathrm{PL}} = f \cdot U_{\mathrm{DP}} \tag{6}$$

where subscripts DP and PL indicate the design point and part load values, respectively. The approach to calculate f is described in the appendix. Once the overall heat transfer coefficient is known, the mean temperature difference in part load $\Delta T^*_{\mathrm{m,PL}}$ can then be found using Eq. (3) with $U_{\mathrm{PL}}A$ and Q_{PL}. When simulating the cycle, the temperature profile and hence the UA value for each heat exchanger can be calculated using the method described in Section 2.1.1. This value is used to calculate the mean temperature difference $\Delta T_{\mathrm{m,PL}}$ for the heat exchanger using Eq. (3). The goal of part load simulations is to ensure that this $\Delta T_{\mathrm{m,PL}}$ converges to $\Delta T^*_{\mathrm{m,PL}}$. To this end the PSO-algorithm mentioned above is used together with a penalty function similar to Eq. (5), which vanishes as $\Delta T_{\mathrm{m,PL}} \rightarrow \Delta T^*_{\mathrm{m,PL}}$. It must be noted that $\Delta T^*_{\mathrm{m,PL}}$ is not a constant value since f in Eq. (6) will change with the mass flow rate of the fluids. One needs to keep in mind that the calculated values of U_{PL} in the current methodology are accompanied by certain simplifications as detailed heat transfer calculations are out of the present scope. While this is not expected to affect the generality of the findings, the results should be interpreted as quantitatively approximate.

3. Results and discussion

3.1. Design point

In Fig. 3, optimal performance of SC-SGHX cycle is illustrated for different mixtures at studied range of temperatures. Each mixture is optimized at different mass fractions with intervals of 0.1. As mentioned before, in the optimization of cycles, the objective is to maximize the COP and the optimization variables are the pressure of condenser, evaporator and separator as well as the superheat level. From Fig. 3 it is clear that mixtures outperform the pure fluids, except for the CO_2/Propane mixture at certain ratios. This is especially the case when large glides are present. This observation is in line with what reported in the previous studies (Zühlsdorf et al., 2018a,c; Yelishala et al., 2020b). While a direct comparison with the data from literature would require identical cycle architecture and sink/source temperature profiles, which is not the case, the current results lie in the expected range considering similar studies. For example Zühlsdorf et al. (2018a) reported the peak COP value for the DME/Iso-Penthane mixtures with 20 K glide on the source side to be between roughly 5.2 and 5.5 depending on the superheat constraints. This value is 5.58 for the same source temperature glide in our study. For the Propylene/Iso-Butane mixture, COP values between 4.6 and 4.7 are reported in the same reference, comparable to the 4.65 in the present work. Notably, in the present study Propylene/Iso-Butane is the least sensitive mixture to a change in its composition, which is similar to the trend observed by Zühlsdrof and co-workers. In Temperature Case 1 (and 2, not shown for brevity) there is a significant difference between the performance of different mixtures. The difference is less pronounced in Temperature Case 3 except for CO_2/Propane mixture.

In Fig. 3(b) it is illustrated that the COP of CO_2/Propane mixture increases from 0.6/0.4 to 0.8/0.2 and hereafter it decreases again. Similar behavior is also observed by previous researchers e.g. in Zühlsdorf et al. (2018a,c), Yelishala et al. (2020a). The reason for this behavior is that with a CO_2 mass fraction of 0.6 the highest pressure in the cycles exceeds the critical value. Such transition into a transcritical cycle leads to a better temperature glide match between mixture

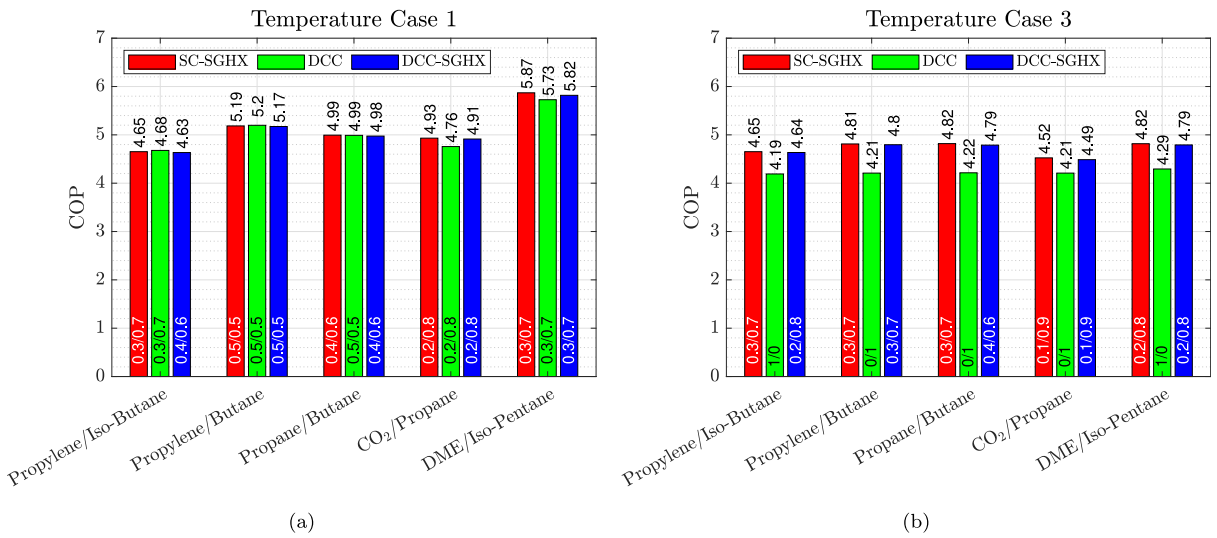

Fig. 5. Comparison of the systems' maximum performance at Temperature Cases 1 and 3 (case 2, not shown for brevity, conforms to the general trend). The value in the bottom of the bars indicates the mass fraction composition of the optimal solution (ODPR).

and heat sink and source, hence the increase in the COP. The best temperature match for the trans-critical cycle is reached at 0.8 CO_2, which corresponds to the second peak observed in the figure.

One must note that while COP controls the energy efficiency, and hence, the running cost of the heat pump, the overall cost of heating is also impacted by the unit price, which, among others, is related to the size of the components. Hence in Fig. 4 we present the volumetric heating capacity (VHC) as a function of mixture mass fraction. VHC is defined as the heating capacity in the condenser per unit volume of working fluid at compressor suction. The results are presented for Temperature Case 3 as a representative example. It is clear that CO_2/Propane has a superior VHC compared to all other cycles, particularly when the CO2 ratio in the mixture is high. This can be an argument in favor of using CO_2-based mixtures for heat pumps. All mixtures not including DME have very similar VHCs. DME/Iso-Pentane is the mixture with the lowest VHC. Despite the fact that this mixture often performs the best in terms of COP, the low VHC, and as a result, large component size can be a barrier in use of this mixture.

The same optimization procedure is repeated for the other two cycles but not reflected in Fig. 3 as, for the reasons explained in the following, the rest of this study is mainly focused on the SC-SGHX cycle. In Fig. 5, optimal performance of all cycle layouts is presented only at the optimum design point mass fraction ratio (ODPR), i.e. the mass fraction ratio for a given mixture and Temperature Case that yields the highest COP. In other words, ODPR corresponds to the peaks of different curves in Fig. 3. Fig. 5 shows that inclusion of intermediate pressure vessels does not meaningfully enhance the performance, as the performance of SC-SGHX is at least equal to that of the DCC and DCC-SGHX for all mixtures and all Temperature Cases. It is furthermore noted that with decreasing glide on the source, from Temperature Case 1 to Temperature Case 3, the performance of the DCC is more severely affected than the other system designs. This is caused by an increasing mismatch of the temperature profiles in the evaporator; for the SC-SGHX and the DCC-SGHX cycles, the working fluid is superheated in the SGHX. However for the DCC cycle, a superheat of 10 K has to take place inside the evaporator. This ends up forcing the evaporating pressure down, when the temperature glide on the source decreases. This results in an increased pressure ratio and thereby decreases the COP for the DCC compared to the other cycles.

3.2. Part load

The results in the previous section indicate that including an intermediate pressure vessel is unlikely to deliver a kind of gain in COP that justifies addition of extra components. In light of this finding, part load simulations are only conducted for SC-SGHX. Initially, we study different part load scenarios for the optimum design point mass fraction ratio (ODPR), i.e. at the mass fractions corresponding to peaks in Fig. 3.

Fig. 6 presents the results for the part load simulation based on Temperature Case 1. In Fig. 6(a) the behavior in Part Load Scenario 1 is studied. In this scenario, all mixtures have a decreasing COP when the heat load is reduced. DME/Iso-Pentane is observed to be the one with the largest decrease. As shown in Fig. 6(b) Part Load Scenario 2 leads to a very different behavior. Here most mixtures show an increase in COP when the load decreases. Only CO_2/Propane and DME/Iso-Pentane behave in a rather peculiar way and show maxima at about 70% heat load. This is due to what happens in the evaporator when the source outlet temperature increases. In this scenario, as the heat load decreases, the pinch point moves towards the outlet of the evaporator on the working fluid side due to the large temperature glide. At a certain load, the pinch occurs at the outlet, which means that a further increase in the source outlet temperature will not yield a higher evaporator pressure. With the condenser pressure still increasing due to increasing sink inlet temperature, the pressure ratio becomes larger and hence a decrease in COP is observed.

This is better illustrated in Fig. 7 where the *T,h*-diagram for the solution of DME/Iso-Pentane at 70% heat load is depicted. In this case, there is a good temperature match in the evaporator with the pinch point occurring fairly midway between the inlet and outlet of the evaporator on the working fluid side. A further reduction of the heat load means an increasing source inlet temperature. Since the mixture has a large temperature glide it means that the pinch point will move towards the outlet of the evaporator. As the pinch point is at the outlet the evaporator pressure cannot increase further and since the sink inlet temperature still is increasing the COP will decrease. This is not an issue for the other mixtures which is why their COP keeps increasing towards lower loads.

For Part Load Scenario 3, as shown in Fig. 6(c), all mixtures undergo a decrease in the COP similar to Scenario 1, with DME/Iso-Pentane being the best performing. In Part Load Scenario 4 as shown in Fig. 6(d) all mixtures have a small increase in COP towards part loads. Fig. 6(e) demonstrates Part Load Scenario 5 where the mixtures have a decreasing COP although for Propylene/Iso-Butane it is a very mild decrease. Notably in all scenarios DME/Iso-Pentane remains to be the best performing mixture in terms of COP down to 40% load.

Generally Fig. 6 shows clearly that mixtures have a higher performance than pure propane in part load. This behavior is believed to

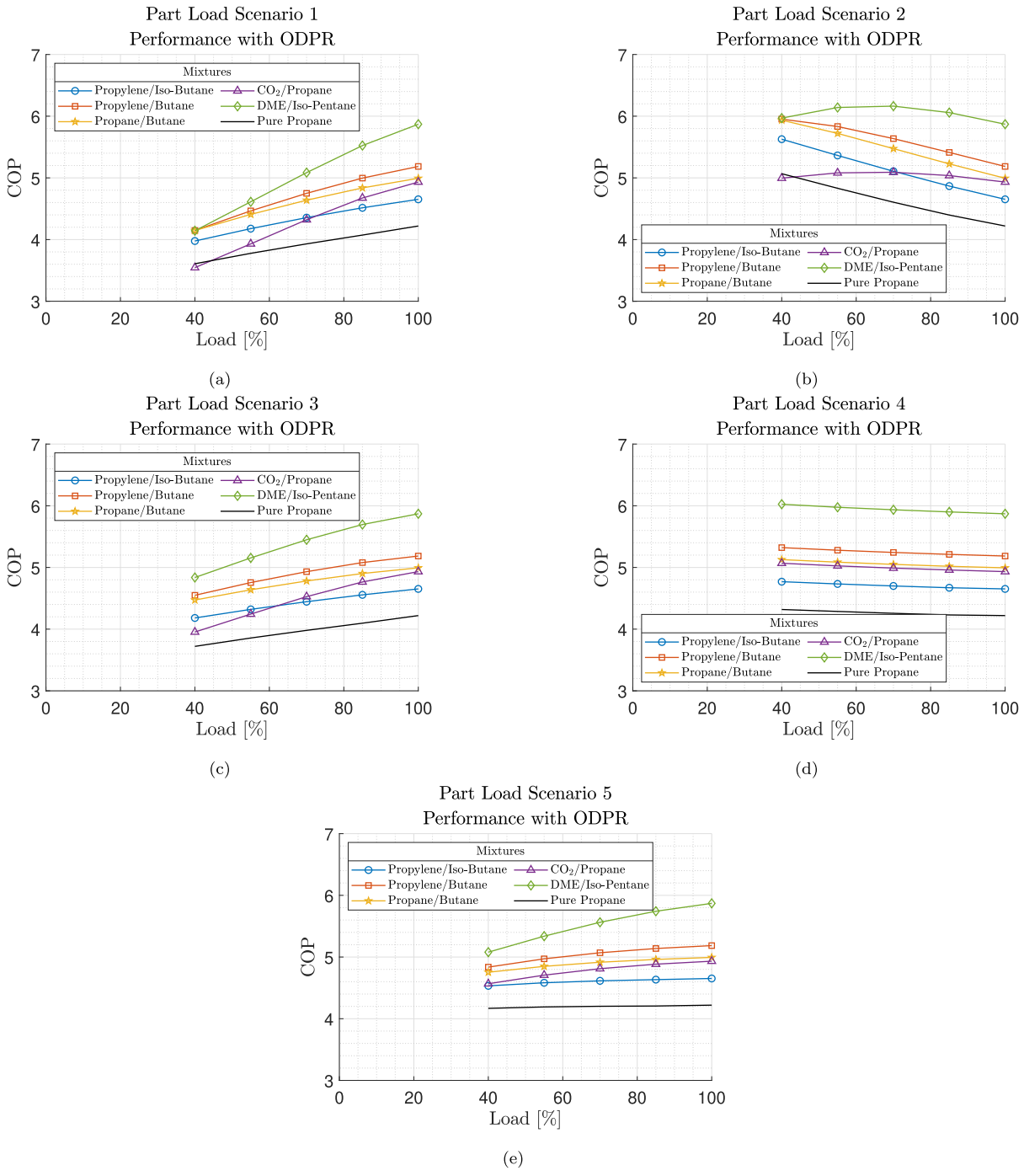

Fig. 6. Comparison of mixtures operating at part load. Mixture ratios are ODPR, equal to the ones shown in Fig. 5(a). Part load simulation is based on Temperature Case 1 presented in Table 3.

be similar for the other pure fluids used in this study. A deviation is CO_2/Propane which in Fig. 6(b) is illustrated to have a lower COP than pure Propane, when the heat load is 40%. Although, similar to the design point optimization, DME/Iso-Pentane is the mixture with the highest COP, it is also evident that different mixtures show different sensitivities to a decrease in the heat load.

To better observe this behavior, in Fig. 8 the change in the COP of each mixture in different part load scenarios is indicated by vertical bars. Here DME/Iso-Pentane clearly shows the largest decrease in COP when the heat load is reduced to 40% of the design load. In Part Load Scenario 1 and 2 DME/Iso-Pentane at 40% heat load has a similar performance to that of Propane/Butane and Propylene/Butane. CO_2/Propane is also observed to have a large decrease in COP when the heat load is reduced. Even though DME/Iso-Pentane is the mixture most affected by decreasing heat load it is still the best performing mixture in all part load scenarios. Table 5 presents the COP for the mixtures at 100%-load and 40%-load along with the difference between the two load cases. We repeated the analysis for other Temperature Cases, and less sensitivity to load reduction is observed; hence, those cases are not shown for brevity.

The results shown in Fig. 6 are with the ODPR for each mixture. However, whether this mixture ratio is also the optimum one at part load is an open question that needs to be addressed. To this end, the part load simulation is also conducted with different mass fraction

Table 5
Change in COP when going from 100% load to 40% load. These results are for ODPR based on Temperature Case 1 from Table 3.

Mixture	Case	PL1	PL2	PL3	PL4	PL5
Propylene/Iso-Butane	Full load	4.65 for all				
	40% load	3.98	5.63	4.18	4.77	4.53
	Difference [%]	−14.5	20.9	−10.1	2.5	−2.6
Propylene/Butane	Full load	5.19 for all				
	40% load	4.15	5.95	4.55	5.32	4.84
	Difference [%]	−20	14.8	−12.3	2.6	−6.7
Propane/ Butane	Full load	4.99 for all				
	40% load	4.15	5.94	4.47	5.13	4.75
	Difference [%]	−17	18.9	−10.4	2.7	−4.8
CO2/Propane	Full load	4.93 for all				
	40% load	3.54	5	3.95	5.07	4.57
	Difference [%]	−28.1	1.3	−19.9	2.8	−7.4
DME/Iso-Pentane	Full load	5.87 for all				
	40% load	4.14	5.97	4.84	6.03	5.08
	Difference [%]	−29.4	1.7	−17.6	2.6	−13.5
Propane	Full load	4.22 for all				
	40% load	3.61	5.07	3.72	4.32	4.17
	Difference [%]	−14.5	20.1	−11.8	2.3	−1.2

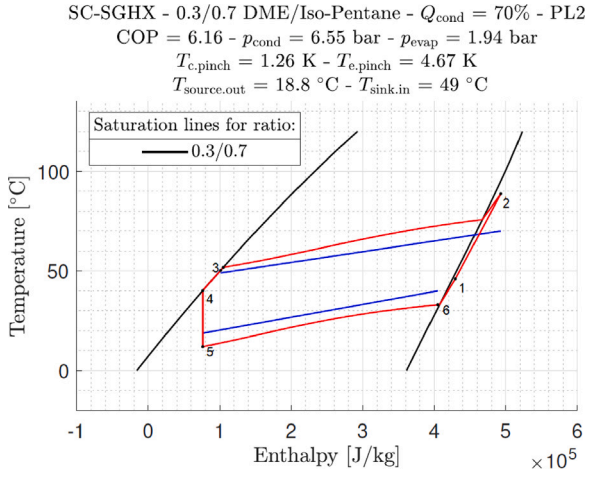

Fig. 7. *T,h*-diagram for DME/Iso-Pentane with 70% heat load in Part Load Scenario 2. The simulation is based on the result from Temperature Case 1 shown in Table 3. The red lines mark the states of the refrigerant in the cycle. The blue lines are the temperature profiles of the heat sink and source . (For interpretation of the references to color in this figure legend, the reader is referred to the web version of this article.)

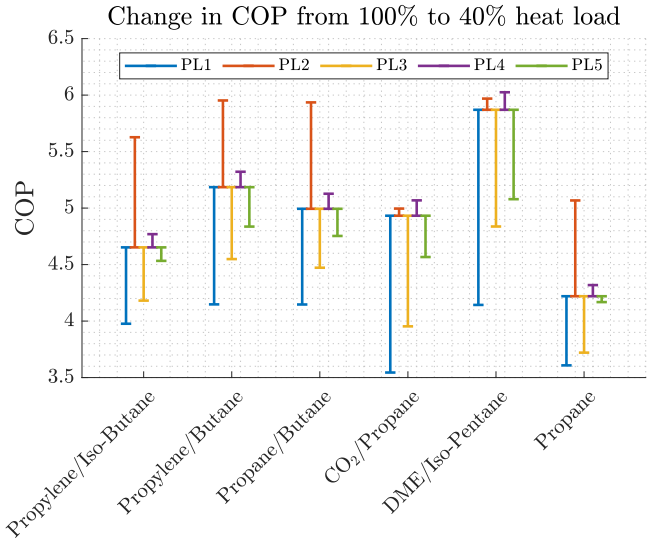

Fig. 8. Change in COP of different mixtures from full load to 40% part load at different part load scenarios for SC-SGHX. Results are presented for Temperature Case 1 (see Table 3) with ODPR. The different Part Load Scenarios (PL) can be found in Table 4.

compositions to investigate if another composition is more optimal to use in part load. Here we focus on Temperature Case 1.

Fig. 9 presents some of the results for Part Load Scenario 2. A case representing the general behavior for all Part Load Scenarios and mixtures is shown by Fig. 9(a) where the ODPR, marked by the yellow line, is also the optimum composition at part load. However, as illustrated by Figs. 9(b) and 9(c) the ODPR is in some cases not the optimum composition. This is especially the case at low heat loads. As shown in Fig. 9(b), for CO_2/Propane different mixture ratios show considerably different trends and ODPR is not necessarily the optimum ratio in part load. For DME/Iso-Pentane the trend is similar for most compositions except the one with 10% DME, as shown in Fig. 9(c). In Fig. 9 the performance for pure propane is also shown.

4. Conclusion

Performance of heat pumps with zeotropic mixtures of natural refrigerants is analyzed in full and different part load conditions. The study is focused on five binary mixtures chosen based on the previous studies. Three different cycle architectures are optimized at full load; these are standard cycle with suction gas heat exchanger (SC-SGHX), double compression cycle without (DCC) and with suction gas heat exchanger (DCC-SGHX). From the design point optimization, it is found that the simplest cycle layout – the SC-SGHX – has virtually the same performance as the best of the other two cycles. The inclusion of an intermediate pressure vessel is therefore not found to be an advantage.

The SC-SGHX cycle is furthermore analyzed in five different part load scenarios at the optimum mass fraction ratio (ODPR) calculated at full load. It is observed that in certain part load scenarios (1, 3 and 5 in Table 4) all mixtures show a decrease in COP, while in some other scenarios (2 and 4 in Table 4) most mixtures show an increase in COP when the load is decreased. CO_2/Propane and DME/Iso-Pentane in Part Load Scenario 2 are the exceptions to the general behavior. Notably, different mixtures show different sensitivities to part load conditions. Among all mixtures under investigation, DME/Iso-Pentane, while delivering the largest COP in both full and part load cases, is most negatively affected by part load performance. As a result, this mixture can be expected to lose its benefit margin over other candidates at part load.

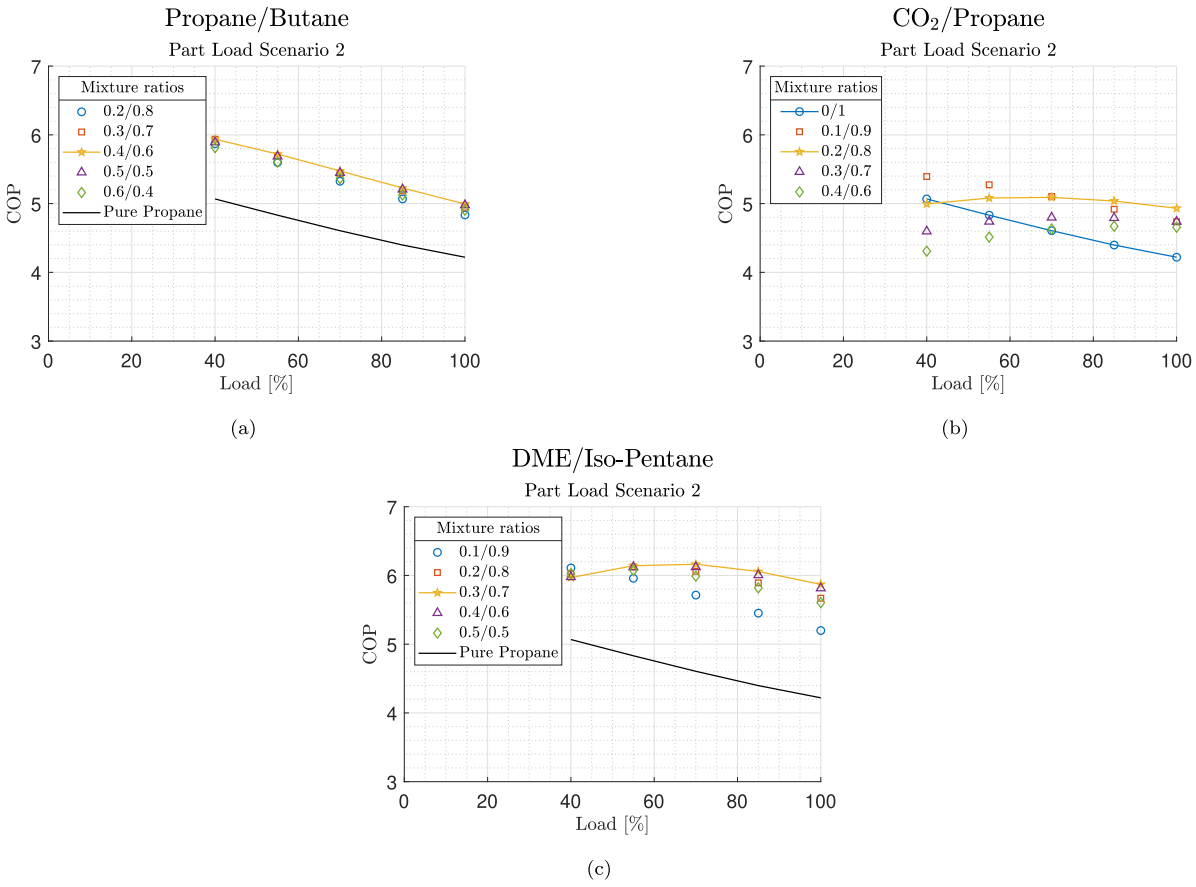

Fig. 9. Performance with different mass fraction compositions in Part Load Scenario 2. The yellow line marks ODPR. (For interpretation of the references to color in this figure legend, the reader is referred to the web version of this article.)

Furthermore, the problem is studied at mixture ratios other than the ODPR. Generally speaking, the ODPR is also the optimum ratio in different part load scenarios but there can be exceptions to this rule, hence care must be taken. Finally, it can be stated that, in the conditions of interest in the present study, mixtures outperform pure fluids not only at design load but also at part load.

Overall, the results point towards the fact that part load performance needs to be taken into account in the design and selection of a heat pump if the system is expected to perform for a significant portion of its lifetime under such conditions as the COP can significantly vary with the load and can depend on the adopted scenario. Moreover, for mixture-based heat pumps, the optimal mixture composition may vary with load.

One must note that the present study only focuses on a certain combination of sink temperatures (40 °C/70 °C) while the effect of sink temperature profile, particularly the case of large supply temperature, can be a direction for future studies. Moreover, one needs to keep in mind that certain simplifying assumptions are incorporated into the present methodology. While this is not expected to affect the generality of the findings, the results should not be interpreted as exact in a quantitative sense.

Declaration of competing interest

The authors declare that they have no known competing financial interests or personal relationships that could have appeared to influence the work reported in this paper.

Acknowledgment

Financial support by Denmark's Energy Technology Development and Demonstration Programme (EUDP) under the project CO2MIX4 Heat is gratefully acknowledged.

Appendix A. Heat transfer coefficients

An estimation of overall heat transfer coefficient in heat exchangers is required to close the part load simulations. The present work aims to provide a general understanding rather than focusing on a specific heat exchanger design. To this end, a number of generic assumptions are used to make an approximate estimation of f in Eq. (6). Firstly, both conductive and fouling thermal resistances in the heat exchangers are neglected. Furthermore, it is assumed that, at design point, convective heat transfer coefficients on the two sides of all heat exchangers are equal. To determine the change in the heat transfer coefficients at part load a simplified approach is followed, where common correlations for heat transfer of zeotropic mixtures in horizontal tubes are used. Here only the effect of changes of mass flow rate on Reynolds number and Froude number are taken into account. It is also assumed that mass flux G changes linearly proportional to the mass flow rate.

For evaporator calculations, we adopt correlation suggested by Zhang et al. (2019) for flow boiling of zeotropic mixtures in horizontal tubes. This correlation is based on dimensionless analysis and multiple regression, where data from other research groups is used as input. Since $T^* = \frac{T_{glide}}{T_{sat}}$ is mostly smaller than 0.06 for the mixtures investigated in this project, Eq. 35 from Zhang et al. (2019) is used to estimate on the refrigerant side. As mentioned, only the terms containing the

mass flux G will be taken into account, as it is assumed that fluid properties are constant. It is also assumed that q will change approximately linearly with G, which means the boiling number Bo is without influence. Applying simplifications, the following proportionality can be achieved for variation of heat transfer coefficient with mass flow of the working fluid.

$$\alpha_{evap} \sim \dot{m}_{WF}^{1.1132} \tag{A.1}$$

Deng et al. (2019) comprehensively discussed condensation heat transfer coefficients of zeotropic mixtures, which is the basis for our condenser calculations. It is possible to calculate the effective condensation heat transfer coefficient, α_{cond} using Bell and Ghaly correction, which can be simplified to

$$\frac{1}{\alpha_{cond}} = \frac{1}{\alpha_p} + x c_{p,v} \frac{T_{glide}}{\Delta h} \frac{1}{\alpha_v} \tag{A.2}$$

where α_p is the heat transfer coefficient based on pure fluid correlations evaluated at properties of the mixture, α_v represents the heat transfer coefficient for the vapor part, x is the vapor quality, T_{glide} is the temperature glide during condensation, Δh is enthalpy change during condensation, and $c_{p,v}$ is the specific heat capacity of the vapor phase (Deng et al., 2019). α_p can be determined by the relation proposed by Cavallini et al. (also described in Deng et al. (2019)). In this model the heat transfer coefficient during condensation is divided into two sections; (1) a ΔT-dependent regime characterized by a progressive change from fully-stratified to annular flow and (2) a ΔT-independent regime characterized by annular flow. Assuming that the condensation process is dominated by annular flow the correlation for α_A in Deng et al. (2019) is valid in most of the condensation process, it is found that $\alpha_p \sim \dot{m}_{WF}^{0.8}$ in Eq. (A.2). For single-phase flows of the zeotropic mixtures (superheated vapor and subcooled liquid), the heat transfer correlations can be estimated using the correlations for pure fluids evaluated with the properties of the mixtures (Radermacher and Hwang, 2005). Therefore, the Dittus Boelter correlation presented in Deng et al. (2019) can be used to estimate α_v. This yields that $\alpha_v \sim \dot{m}_{WF}^{0.8}$ in Eq. (A.2).

Since both α_v and α_p roughly scales with the $\dot{m}_{WF}$ to the power 0.8 the following expression can be established.

$$\alpha_{cond} \sim \dot{m}_{WF}^{0.8} \tag{A.3}$$

The heat transfer coefficients on both sides of the SGHX and on the on water side of the evaporator and condenser can be determined using the Dittus–Boelter correlation, which yields:

$$\alpha_{SGHX} \sim \dot{m}_{WF}^{0.8} \quad \alpha_{water} \sim \dot{m}_{water}^{0.8} \tag{A.4}$$

Based on the estimated change in the different heat transfer coefficients the reduction factor f can be found.

References

Barco-Burgos, J., Bruno, J., Eicker, U., Saldaña-Robles, A., Alcántar-Camarena, V., 2022. Review on the integration of high-temperature heat pumps in district heating and cooling networks. Energy 239, 122378. http://dx.doi.org/10.1016/j.energy.2021.122378.

Brodal, E., Eiksund, O., 2020. Optimization study of heat pumps using refrigerant blends –Ejector versus expansion valve systems. Int. J. Refrig. 111, 136–146.

Dai, B., Dang, C., Li, M., Tian, H., Ma, Y., 2015. Thermodynamic performance assessment of carbon dioxide blends with low-global warming potential (GWP) working fluids for a heat pump water heater. Int. J. Refrig. 56, 1–14.

Deng, H., Rossato, M., Fernandino, M., Del Col, D., 2019. A new simplified model for condensation heat transfer of zeotropic mixtures inside horizontal tubes. Appl. Therm. Eng. 153, 779–790.

Faegh, M., Shafii, M.B., 2019. Performance evaluation of a novel compact humidification-dehumidification desalination system coupled with a heat pump for design and off-design conditions. Energy Convers. Manage. 194, 160–172. http://dx.doi.org/10.1016/j.enconman.2019.04.079.

Guo, H., Gong, M., Qin, X., 2019. Performance analysis of a modified subcritical zeotropic mixture recuperative high-temperature heat pump. Appl. Energy 237, 338–352.

Jung, D., Kim, H.-J., Kim, O., 1999. A study on the performance of multi-stage heat pumps using mixtures. Int. J. Refrig. 22 (5), 402–413.

Kim, J.H., Cho, J.M., Kim, M.S., 2008. Cooling performance of several CO_2/propane mixtures and glide matching with secondary heat transfer fluid. Int. J. Refrig. 31, 800–806.

Lemmon, E.W., Bell, I.H., Huber, M.L., McLinden, M.O., 2018. NIST standard reference database 23: Reference fluid thermodynamic and transport properties-REFPROP, version 9.0, national institute of standards and technology. http://dx.doi.org/10.18434/T4/1502528, URL https://www.nist.gov/srd/refprop.

Madsen, C., Kristófersson, J., Murphy, C., Zühlsdorf, B., Olsen, L., Elmegaard, B., Markussen, W.B., Jensen, J.K., 2019. Mixed refrigerant heat pumps/cooling systems (MIREHP) Final report. Tech. rep., Danish Technological Institute and Technical University of Denmark.

Mohanraj, M., Muraleedharan, C., Jayaraj, S., 2011. A review on recent developments in new refrigerant mixtures for vapour compression-based refrigeration, air-conditioning and heat pump units. Int. J. Energy Res. 35, 647–669.

Nocedal, J., Wright, S.J., 2006. Numerical Optimization, second ed. Springer Science & Business Media, ISBN: 978-0387-30303-1.

Park, K.-J., Jung, D., 2009. Performance of heat pumps charged with R170/R290 mixture. Appl. Energy 86, 2598–2603.

Pieper, H., Krupenski, I., Brix Markussen, W., Ommen, T., Siirde, A., Volkova, A., 2021. Method of linear approximation of COP for heat pumps and chillers based on thermodynamic modelling and off-design operation. Energy 230, 120743. http://dx.doi.org/10.1016/j.energy.2021.120743.

Radermacher, R., Hwang, Y., 2005. Vapor Compression Heat Pumps: With Refrigerant Mixtures, first ed. CRC Press, ISBN: 0-8493-3489-6.

Rajapaksha, L., 2007. Influence of special attributes of zeotropic refrigerant mixtures on design and operation of vapour compression refrigeration and heat pump systems. Energy Convers. Manage. 48 (2), 539–545.

Sahin, E., Adiguzel, N., 2022. Experimental analysis of the effects of climate conditions on heat pump system performance. Energy 243, 123037. http://dx.doi.org/10.1016/j.energy.2021.123037.

Sarkar, J., 2010. Review on cycle modifications of transcritical CO_2 refrigeration and heat pump systems. Adv. Res. Mech. Eng. 1, 22–29.

Sarkar, J., Bhattacharyya, S., 2009. Assessment of blends of CO_2 with butane and isobutane as working fluids for heat pump applications. Int. J. Therm. Sci. 489, 1460–1465.

Shariatzadeh, O.J., Abolhassani, S., Rahmani, M., Nejad, M.Z., 2016. Comparison of transcritical CO2 refrigeration cycle with expander and throttling valve including/excluding internal heat exchanger: Exergy and energy points of view. Appl. Therm. Eng. 93, 779–787. http://dx.doi.org/10.1016/j.applthermaleng.2015.09.017.

Tan, Z., Feng, X., Wang, Y., 2021. Performance comparison of different heat pumps in low-temperature waste heat recovery. Renew. Sustain. Energy Rev. 152, 111634. http://dx.doi.org/10.1016/j.rser.2021.111634.

The MathWorks Inc., 2021. Particleswarm. URL https://se.mathworks.com/help/gads/particleswarm.html, Visited: 13-10-2021.

United Nations, 1987. The montreal protocol on substances that deplete the ozone layer.

United Nations, 1998. Kyoto protocol to the united nations framework convention on climate change.

Wang, D., Chen, Z., Gu, Z., Liu, Y., Kou, Z., Tao, L., 2020a. Performance analysis and comprehensive comparison between CO_2 and CO_2 /ethane azeotropy mixture as a refrigerant used in single-stage and two-stage vapor compression transcritical cycles. Int. J. Refrig. Journal 115, p. 39–47.

Wang, Z., Lu, Z., Yelishala, S.C., Metghalchi, H., Levendis, Y.A., 2020b. Laminar burning speeds and flame instabilities of isobutane carbon dioxide air mixtures at high pressures and temperatures. Fuel 268, 117410.

Wang, Z., Lu, Z., Yelishala, S.C., Metghalchi, H., Levendis, Y.A., 2021. Flame characteristics of propane-air-carbon dioxide blends at elevated temperatures and pressures. Energy 228, 120624.

Xiao, B., Chang, H., He, L., Zhao, S., Shu, S., 2020. Annual performance analysis of an air source heat pump water heater using a new eco-friendly refrigerant mixture as an alternative to R134a. Renew. Energy 147, 2013–2023.

Yelishala, S.C., Kannaiyan, K., Wang, Z., Metghalchi, H., Levendis, Y.A., Sadr, R., 2020a. Performance maximization by temperature glide matching in energy exchangers of cooling systems operating with natural hydrocarbon/CO_2 refrigerants. Int. J. Refrig. 119, 294–304.

Yelishala, S.C., Kannaiyan, K., Wang, Z., Metghalchi, H., Levendis, Y.A., Sadr, R., 2020b. Thermodynamic study on blends of hydrocarbons and carbon dioxide as zeotropic refrigerants. J. Energy Resour. Technol. 142 (8), 082304.

Yu, B., Liu, D.W.C., Jiang, F., Shi, J., Chen, J., 2018. Performance improvements evaluation of an automobile air conditioning system using CO_2/propane mixture as a refrigerant. Int. J. Refrig. 88, 172–181.

Zhang, J., Mondejar, M.E., Haglind, F., 2019. General heat transfer correlations for flow boiling of zeotropic mixtures in horizontal plain tubes. Appl. Therm. Eng. 150, 824–839.

Zhang, X., Wang, F., Fan, X., Duan, H., Zhu, F., 2017. An investigation of a heat pump system using CO2/propane mixture as a working fluid. Int. J. Green Energy 14 (1), 105–111. http://dx.doi.org/10.1080/15435075.2016.1253577.

Zühlsdorf, B., Jensen, J.K., Cignitti, S., Madsen, C., Elmegaard, B., 2018a. Analysis of temperature glide matching of heat pumps with zeotropic working fluid mixtures for different temperature glides. Energy 153, 650–660.

Zühlsdorf, B., Jensen, J.K., Elmegaard, B., 2018b. Numerical models for the design and analysis of heat pumps with zeotropic mixtures. https://figshare.com/s/575b3a3760275aee119e, Visited: 19-03-2021.

Zühlsdorf, B., Jensen, J.K., Elmegaard, B., 2019. Heat pump working fluid selection—economic and thermodynamic comparison of criteria and boundary conditions. Int. J. Refrig. 98, 500–513.

Zühlsdorf, B., Meesenburg, W., Ommen, T.S., Thorsen, J.E., Markussen, W.B., Elmegaard, B., 2018c. Improving the performance of booster heat pumps using zeotropic mixtures. Energy 154, 390–402.